Accepted Manuscript

Title: Identifying central and peripheral nerve fibres with an artificial intelligence approach

Author: David Gil Jose Luis Girela Jorge Azorín Alba De Juan Joaquin De Juan
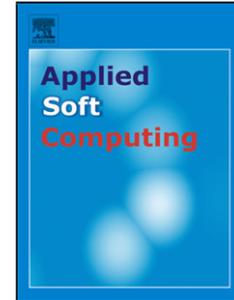
Please cite this article as: David Gil, Jose Luis Girela, Jorge Azorín, Alba De Juan, Joaquin De Juan, Identifying central and peripheral nerve fibres with an artificial intelligence approach, *<![CDATA[Applied Soft Computing Journal]]>* (2018), https://doi.org/10.1016/j.asoc.2018.03.010

This is a PDF file of an unedited manuscript that has been accepted for publication. As a service to our customers we are providing this early version of the manuscript. The manuscript will undergo copyediting, typesetting, and review of the resulting proof before it is published in its final form. Please note that during the production process errors may be discovered which could affect the content, and all legal disclaimers that apply to the journal pertain.

Identifying central and peripheral nerve fibres with an artificial intelligence approach

David Gil[a,*], Jose Luis Girela[b], Jorge Azorín[a], Alba De Juan[b], Joaquin De Juan[b]

[a]*Computing Technology and Data Processing, University of Alicante, Spain*
[b]*Department of Biotechnology, University of Alicante, Spain*

Abstract

Distinguishing axons from central or peripheral nervous systems (CNS or PNS, respectively) is often a complicated task. The main objective of this work was to facilitate and support the process of automatically distinguishing the different types of nerve fibres by analysing their morphological characteristics. Our approach was based on a multi-level hierarchical classifier architecture that can handle the complexity of directly identifying nerve-fibre groups belonging to either the CNS or the PNS. The approach adopted comprises supervised methods (multilayer perceptron and decision trees), which are responsible for distinguishing the origin of the axons (CNS or PNS), whereas the unsupervised method (K-Means clustering) performs nerve fibre clustering based on similar characteristics for both the CNS and PNS. Our experiments produced results with an accuracy higher than 88%. Our findings suggest that the development and implementation of a multi-level system improves automation capabilities and increases accuracy in the classification of nerves. Furthermore, our architecture allows for generalisation and flexibility, which can subsequently be extended to other biological control systems.

Keywords: artificial neural network, k-means clustering, decision trees, decision support system, nerve fibres, multi-level classifier

1. Introduction

The number of published works related to nerve fibres has progressively increased from the beginning of the 20th century as shown in Figure 1. A rapid search in PubMed revealed the publication of approximately 130,000 pertinent papers during this period. Almost 40% of these, approximately 50,600 articles, were published in the first 14 years of the 21st century, with most (78%) in the last ten years.

---

*Corresponding author
Email address: david.gil@ua.es (David Gil)
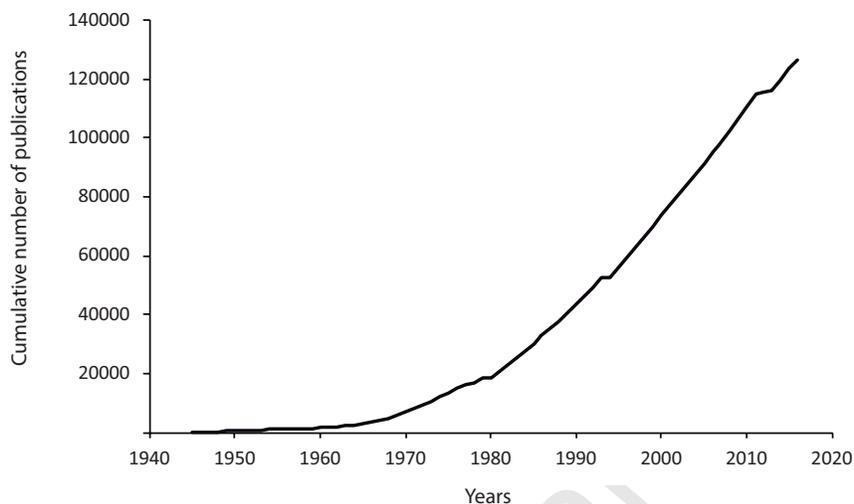
Figure 1: Cumulative number of publications on morphometric research in nerve fibres

The first studies registered in PubMed using morphometric techniques date back to 1969 [1]. Approximately 1600 articles on morphometric research in nerve fibres have been published in the same period, with approximately 30% of these within the last decade. Among them, we could only locate starting in 1969, approximately 400 studies using morphometric methods associated with electron microscopy. Furthermore, publications related to morphometric and ultrastructural studies have been less abundant, especially those related to optic nerve fibres (73 articles) and cochlear nerve fibres (16 articles).

The morphometric study of nerve fibres is a useful approach to research several subjects related to the nervous system, such as development ([2], [3], aging, [4] [5] [6] [7] [8]) and pathological conditions both in peripheral [9] [10] [11] [12] and central nerve fibres [13].

Several morphometric studies have shown a similar relationship between functional features of nerve fibres and their morphological and morphometric parameters, such as (a) number, density, and diameter of nerve fibres [14] [15] [16] [17] [18] [19] [20] [21] [22] [23] (b) in vertebrates, the myelin sheath that encircles large axons determines the fibre conduction velocity. In fact, myelin thickness is related to the speed at which an axon can transmit electrical impulses [24] [25], and for this reason myelin sheath characteristics are also of interest [26] [27] [18] [28] [29] [30] [23] as well as axonal cytoskeletal components [2] [31] [32] [33].

Classically, morphometry was performed manually. However, numerous locations in the nervous system contain exceedingly large numbers of nerve fibres; for example, the rat optic nerve contains more than 100,000 fibres [17] and the human optic nerve more than a million [34] [35] [36]. In these cases, manual

2

morphometry is very monotonous, tiring, time-consuming, and predisposed to error [37]. Hence, researchers have been adopting different analysis systems to study the morphological and morphometric features of nerve fibres [8] [36] [38] [39] in order to significantly reduce data input and processing times. A variety of sampling schemes claim to be capable of resolving this problem and guarantee the reliability of morphometry [37]. Consequently, there is high motivation for for the development of automatic morphometry systems.

The application of automatic image processing in fibre recognition has drawn much attention from the image processing and neurology communities. Morphometry that is entirely automated has certain disadvantages, namely, miss-detection and false positives [37]. This manner of automatization has been previously discussed in the literature in cases where the axon is small, illegible, or irregular and could be undervalued due to low contrast as well as other issues related to the automated identification of contours. [40] [41] [42]. Currently, automatic morphometry combining interactive image processing has made significant progress [43] in terms of miss-detection and false positives.

This paper proposes a multi-level classifier architecture to resolve the complexity of automatically identifying whether a nerve fibre belongs to the central or peripherical nervous system (CNS or PNS). In particular, we used two supervised techniques, multilayer perceptron (MLP) and decision trees (DT), [Polat and Gunes, 2009] and an unsupervised technique, K-Means clustering. The supervised method is responsible for distinguishing the origin of the nerve fibres (CNS versus PNS) whereas the unsupervised one performs the division of clusters or groups with similar characteristics either for the CNS or PNS.

Recently, advances in AI methods have made possible the development of expert and decision support systems (DSS) in many different areas, such as business analytics, medical diagnostics, psychology, and environmental science. Specifically, a review of the evolution of medical data analysis from a machine learning perspective [44] indicates how AI methods have been applied in the medical field. A study by [45] proposed a hybrid artificial intelligence (based on a fuzzy rule-based system) to forecast outpatient visits with high accuracy. In [46], a trained artificial neural network (ANN) model was developed to predict the weekly number of infectious diarrhoeas by using meteorological factors as input variables.

Among the several useful classifiers in the AI field, we highlight ANN and DT as those most frequently chosen for the construction of DSS [47]. The goal is normally to establish groups or clusters with similar features from the data. Since there are no references or expected classification and the classification is data driven, the system is unsupervised.

We have previously demonstrated that AI methods are capable of improving the accuracy of the final classification as well as of selecting the best features because very often there are many features to control. For instance, we have experience in classification tasks for male fertility [48] [49], urology diagnosis [50] [51], and brain ventricles in MR images [52]. In [53], a model to diagnose urological dysfunction is presented. The aim of the study was to correlate the neurological aetiology with the neural centres involved in the two urological

3

phases of voiding and micturition. This previous experience may lead to knowledge discovery regarding databases, data mining, or the process of extracting patterns from large datasets. Nowadays, these techniques are also starting to be used in the field of big data [54] [55].

In the present study, the main objective was to develop a classifier architecture based on AI methods that could distinguish different types of nerves and classify two main types of nerve fibres (CN versus PN nerve fibres).

The novelty and the main contribution of this work is the proposal of a multi-level hierarchical classifier architecture, which comprises supervised as well as unsupervised methods. The hierarchical classifier simplifies the complexity of identifying whether a nerve fibre belongs to the CNS or the PNS and their respective characteristics. Moreover, it allows using different classification methods according to the specific semantic level by providing a flexible approach.

In general, a multi-level hierarchical architecture provides the benefit of a classification where the number of variables is reduced from the higher to the lower levels of the system. Hence, the classifiers for lower levels could be simpler due to reduction in the variable domain. However, in the case of a complex problem, it is not always possible to select the variables that allow the specification of a detailed taxonomy. Finally, the multi-level architecture allows for the selection of the most appropriate classification for the study of the problem in terms of resolution level. Therefore, this approach could be used to study other biological problems.

This work was concerned with the most relevant parameters for both optic and cochlear nerve fibres. The number of parameters is often large and therefore, weighing is crucial to choose only key parameters involved in the classification process of nerve fibres. The approach chosen to address this issue involved using different AI methods that are both supervised and unsupervised, specifically DT, MLP, and unsupervised k-means. The general differences between central and peripheral nerve fibres are well known, and a trained pathologist can distinguish between them easily under the microscope. Nevertheless, the advantage of this approach is the possibility of automating the identification procedure. In addition, it allowed us to identify the hierarchy present in the characteristics of each fibre, providing a new interpretation of the evolution and development of the nervous system.

The remaining part of the paper is organized as follows: First we start by defining the materials and methods of the study (samples of the study). Then, we continue with a brief description of the AI methods used in this paper: MLP, DT, and K-means. Then we proceed by describing the design of our proposed architecture and the experiments carried out in the Results section: the available data as well as a detailed explanation of the different values of our database. Finally, we describe the subsequent testing carried out to analyse the results and draw relevant conclusions.

4

2. A bio-inspired multi-level classifier of nerve fibres

2.1. Architecture

A generic machine learning approach is able to extract a model from data to predict or classify new inputs. Hence, a classifier could be designed using machine learning techniques to learn the type of fibre characteristics irrespective of the level of the taxonomy to be applied (i.e. the fibre belongs to the CNS or the PNS, to a cochlear or sciatic nerve, to a sensory or motor fibre, and others). The diagram in Fig. 1 shows the procedure followed to classify the different fibres in the nerves. A tissue is obtained, processed for transmission electron microscopy, and analysed to obtain morphometric parameters (a set of characteristics that describe a fibre) that can be used as input for a single classifier. At Level 1, the classification system can model the type of fibre according to whether it belongs to the CNS or the PNS.
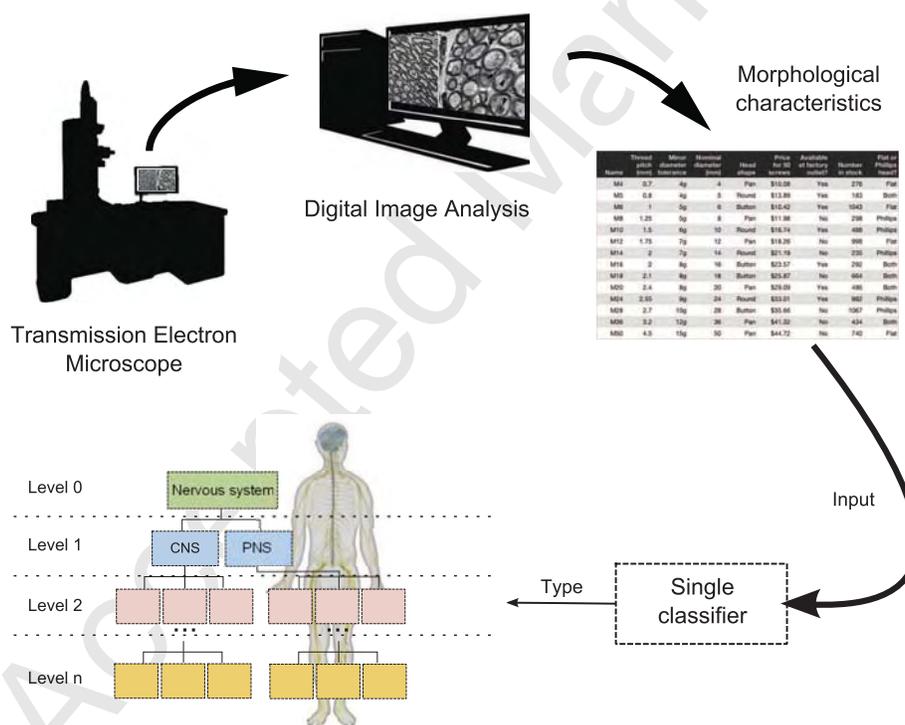
Figure 2: Our proposed multi-level hierarchical classifier

Initially, we carried out some experiments to establish the best approach to group the different types of nerve fibres. We tried to identify the different

5

groups of fibres from the complete set of input data[1]. Although we could observe a general grouping trend between central and peripheral nerve fibres, notably, most of the clusters misclassified a significant number of fibres. To ensure that this was not an exceptional error but a common problem that needed to be addressed, we carried out a second set of experiments with a reduced number of input parameters. The results indicated that in this case the misclassification was worse. Hence, we decided to use the multi-level approach.

The complexity of directly identifying nerve-fibre groups belonging to the CNS or PNS, is due to the similar morphological characteristics of the fibres. Morphological characteristics define similar input samples for different classes making it difficult for a direct classifier to accurately separate them.

The misclassification problem has been addressed by proposing a multi-level hierarchy classifier. The objective is to distinguish the class that the sample belongs to by a process guided by the level of taxonomy. The classifier can identify fibre groups as a generic classifier based on the level of taxonomy (see Fig. 3). It is a bio-inspired system based on the anatomical or functional differences of the nervous system (see Fig. 4). Specifically, the set of fibre characteristics are classified according to the specific level of taxonomy using a hierarchical strategy. The classifier at level L_n uses information derived from the previous level L_{n-1}. This multi-level architecture permits different classification methods to be used accordingly for each specific level, providing a flexible approach. Thus, the most suitable machine learning method is used depending on the expected output. For example, the machine learning approach selected to distinguish between a cochlear or sciatic nerve could be different to the one selected for distinguishing between a sensory or a motor fibre.

The approach based on the multi-level classifier is similar to the deep learning method in the sense that both consist of a multi-level structure to provide a classification. However, while the deep learning method requires thousands of instances to adequately train the network, the proposed approach is designed to train a machine learning system with a low number of samples, as is generally the case with biological problems. In any case, a deep learning method could be incorporated at any level in our approach.
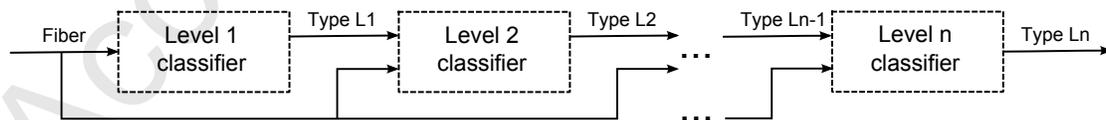
Figure 3: The proposed multi-level hierarchy architecture to classify fibres according to the level of selected taxonomy.

In this work, the objective was to automatically distinguish the different

---

[1]The dataset has been donated to the repository uci machine learning (http://archive.ics.uci.edu/ml/index.php)

6

types of nerve fibres based on their morphological characteristics. The study involved a morphological taxonomy based on two levels: the first level focused on identifying whether the fibre belongs to the CNS or the PNS and the second level used the information obtained from the first level to cluster the fibre types. Figure 4A shows the specific architecture proposed in this paper, where we used the optic nerve as an example of a CNS nerve and the cochlear nerve as an example of a PNS nerve (Figure 4B).
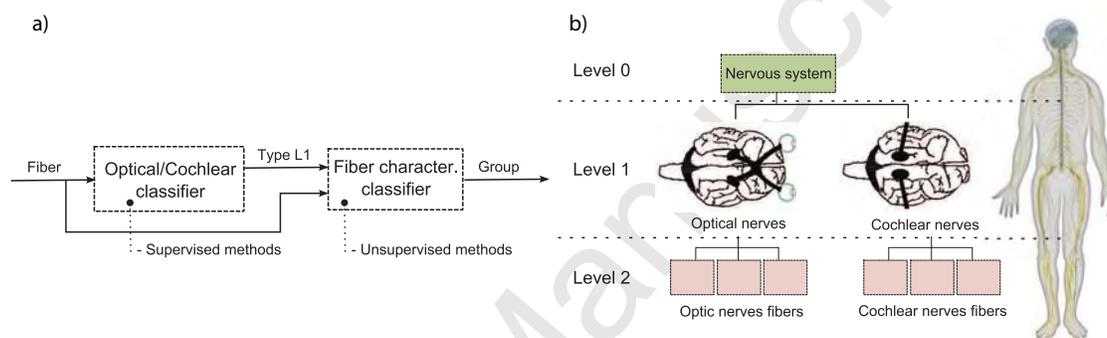
Figure 4: The multi-level architecture used to classify nerve fibres based on the morphological taxonomy.

2.2. Central versus peripheral classifier

In this paper, to evaluate the flexibility provided by the multi-level hierarchical architecture, tests were performed at the first level with two different machine learning classifiers: decision trees and multilayer perceptron. These two methods are the most common techniques of supervised learning. We combined the decision trees and artificial neural networks. On one hand, DT offers the representation of rules, which can be readily understood or used directly in databases. On the other hand, MLP is a bio-inspired method, which is very suitable in this context.

There exist diverse algorithms to represent DT such as [56] C4.5 [57], and CART [58]. The classification and regression trees (CART or C&RT) method of Breiman, Friedman, Olshen, and Stone ([58]) generates binary decision trees. Although real-life scenarios are not always as simple as binaries, binary decision trees are in fact an excellent as well as an easier method of interpreting and analysing the environment ([59] and [60]). Therefore, in our case, we used DT to classify the differences between the optic and cochlear nerves.

An MLP comprises usually three layers of neurons, where every layer is entirely connected to the next one. The first input layer receives external inputs, then one hidden layer (which is the most complex layer as it needs to be configured for and adapted to every situation), and finally, an output layer which achieves the classification results [61] [62][63] (see figure 5).

7
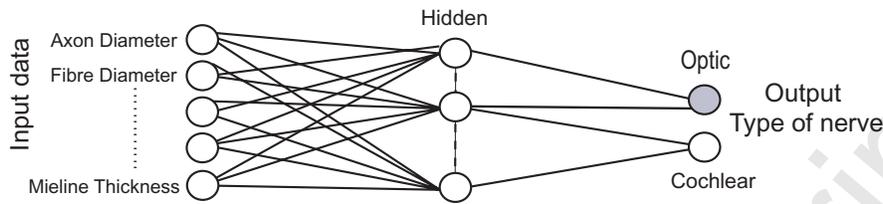
Figure 5: The architecture of the MLP network (input layer, hidden layer, and output layer). The input layer represents the input data (the input dataset is described in section 3.2). The usage of a hidden layer enables the representation of datasets that are not linearly separable. The output layer represents the classification result and it contains as many outputs as the problem has classes. The weights and the threshold of the MLP are calculated during an adaptation process.

The training of the MLP is carried out by backpropagation, which is a supervised learning method. It uses a gradient descent method for the adaptation of the weights. A detailed explanation of this algorithm can be found in [64].

2.3. Fibre type classifier

For the second decision layer, an unsupervised method was used in order to classify the fibre type. Unlike the first level of the taxonomy, the morphological characteristics of the fibres are not well studied. There is no clear consensus regarding the types presented in the nerves. Hence, unsupervised methods will be able to provide knowledge to the biological area since they are able to cluster similar characteristics that cannot be easily extracted by an expert. In this case, an initial study using k-means was considered to be the machine learning method of our hierarchical architecture.

2.3.1. K-Means clustering

Clustering is a process of partitioning or grouping a set of data objects into clusters.

Given a set of observations $(x_1, x_2, ?, x_n)$, where each observation is a d-dimensional real vector, k-means clustering aims to partition the n observations into k sets $(k \leq n)S = S1, S2, ?, Sk$. Assuming an initial set of k means $m1(1), ?, mk(1)$, the algorithm [65] proceeds by alternating between two steps:

- Assignment step: Assign each observation to the cluster whose mean yields the least within-cluster sum of squares. Since the sum of squares is the squared Euclidean distance, this is intuitively the "nearest" mean. (Mathematically, this denotes partitioning the observations according to the Voronoi diagram [66] generated by the means)

8

- Update step: Calculate the new means to be the centroids of the observations in the new clusters.

The algorithm has converged when the assignments no longer change.

There exists extensive literature on algorithms for unsupervised clustering [67], [68], [69] with the k-means method [70] [71] being one of the most popular choices.

Despite the advantages of k-means as a traditional cluster analysis method, this technique is sensitive to the choice of a starting point for partitioning the items into K initial clusters. Due to the weakness of the K-means method, prior literature proposes to adopt a two-staged clustering method [72]. In this regard, this study applied the K-means technique to determine the clustering boundaries from the results of the supervised methods, DT or MLP. In the first stage, a dataset is clustered via adopting the type of nerve to centre the data type to decide the number of data clusters (k). In the second stage, the derived approximation of the clusters (k) determined in the first stage is used with the K-means method.

Finally, in this section, it is interesting to indicate that the method used to evaluate these AI methods was to obtain certain measures to evaluate classification accuracy, sensitivity, specificity, positive rate, negative rate, and a confusion matrix. A confusion matrix [73] contains information regarding actual and predicted classifications performed by a classification system.

3. Computational experiments

In this section, we describe the experiments carried out in order to validate the proposed multi-level architecture, and afterwards, we describe the results obtained. First, we conducted a supervised experimentation to classify between the optic and cochlear nerves as the first level of the architecture. Second, unsupervised experimentation was performed to distinguish the types of fibres within each type of nerve as the second level of the architecture.

3.1. Samples of the study

Optic and cochlear nerves from rat were processed for electron microscopy techniques. Three 1-year-old albino Wistar rats were anesthetized with 35% chloral hydrate (1 ml/kg, i.p) and transcardially perfused with 4% paraformaldehyde, 2% glutaraldehyde in 0.1 M phosphate buffer (pH 7.4). Prechiasmatic portions of the optic nerve and fragments of the cochlear nerve were dissected and maintained overnight in the same fixative at room temperature, post-fixed in 2% OsO4 for 1 h and embedded in Epon 812. In figure 6 are presented the main components of a nerve fibre. One of the main objectives of this work was to discover which are the most important input data correlated with the output.

9
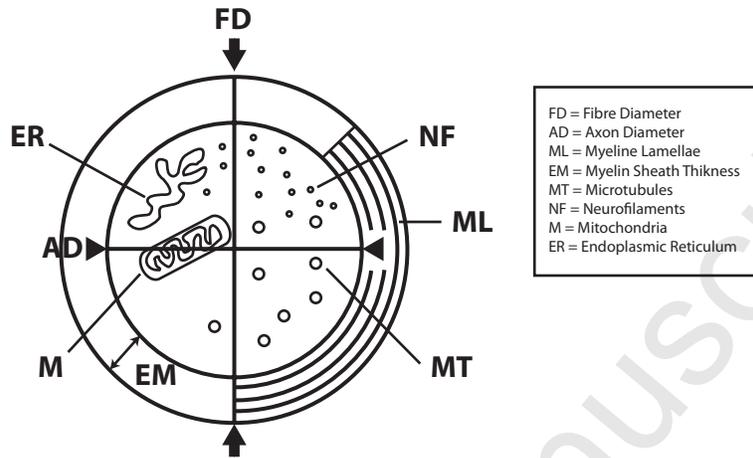
Figure 6: Main components of a nerve fibre.

3.1.1. Morphometry analysis

Electron micrographs were obtained with a ZEISS C-10 electronmicroscope and printed at a final magnification of x 140,000. With the aid of a computer-linked planimeter and a morphometrical package designed by [32]. The following axonal parameters were determined: area of cross-sectioned axons and fibres, number of microtubules and neurofilaments, myelin sheath thickness, and the G-ratio (axon diameter/fibre diameter). These parameters were measured on 100 axons per section randomly chosen from photomicrographs as previously described [2] [17].

3.2. Differences between central and peripheral nerves

In this section, we present the experiments and the results of the supervised experimentation to classify between the optic and cochlear nerves. Of the morphological parameters obtained from the biological samples, we used as input data those indicated in Table 1.

Table 1: Input and output data.

Name	Type
Axon Diameter	Input data
Fibre Diameter	Input data
G-Ratio	Input data
R-Proportion	Input data
Myelin Thickness	Input data
Type of nerve	Output: Optic Nerve = CNS, Cochlear Nerve = PNS

The experimentation was carried out using the WEKA software [74] that contains most of the machine learning techniques.

10
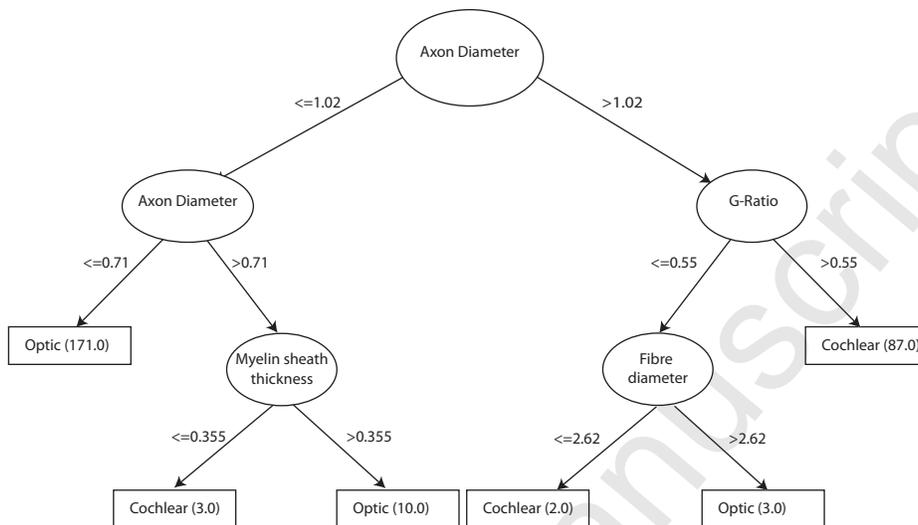
Figure 7: This figure shows the execution carried out with a decision tree. This figure could help establish what are the fields most important for the output.

We used cross-validation as the method to assess the generalization of a network; specifically, for this study we applied a ten-fold cross-validation for the performance assessment. All data were divided into training data (for the process of constructing the model) and test data (data used to validate the model). The baseline experiments were carried out to determine the fibre types without taking into account whether they belonged to the optic or cochlear nerve. The direct clustering for the second level results obtained a 15.6% of instances incorrectly classified. With the proposed architecture, the instances incorrectly classified were reduced to less than 2%.

Figure 7 represents the decision tree of this experimentation. The figure shows the differences to classify between the optic and cochlear nerves and the most important fields to establish the output correlated with the input data. It also shows how the "Axon Diameter" variable performs the first division, which renders it the most important variable. This can also be applied to the remaining features along the tree (G-Ratio, myelin sheath thickness, and fibre diameter).

For the construction of the MLP architecture, we can conclude that layer 1 and 3 are the simplest ones (1 corresponds directly to the input vector and 3 is the output layer with two outputs for classification: central and peripheral nerves. Layer 2 (the hidden layer) consists of the number of hidden neurons and is the most elaborate in the network's architecture. The number of hidden neurons represents a trade-off between performance and the risk of overfitting. In fact, this number will significantly influence the network's ability to general-ize from the training data to unknown examples [75]. To achieve high accuracy

11

without overfitting in order to generalize, the experiments carried out showed that a low number of neurons for this layer resulted in a poor performance for both the training and test datasets. By contrast, a high number of neurons performed very well in the training and test datasets, although the risk of over-fitting was high. The various tests carried out between these extreme options provided us with nine neurons as the optimal solution for this layer. The learning algorithm used was backpropagation with adaptive learning rate, constant momentum, and an optimized algorithm based on the gradient descent method. The backpropagation training parameters are shown in Table 2. We used the default values, except for the parameter epochs, which we tuned to 100, 1000, and 10000 to analyse the different results. All the experiments presented in the tables for MLP were conducted with these parameters.

Table 2: Backpropagation training parameters.

Parameters	Value
Learning rate	0.01
Adaptive learning rate	0.1
Constant momentum	0.2
Epochs	100-1000-10000
Minimum performance gradient	$1e^{-5}$

The results of the experimentation of this first level of supervised classification are shown in Tables 3 and 4. The MLP outperformed the DT. The MLP could classify 98.9% of the samples without false alarms (100% specificity)

Table 3: Definition of the confusion matrix for the central versus peripheral nerve classification with the values for every measure of the MLP and DT classifiers. O = Optic nerve C = Cochlear nerve.

Actual	MLP Predicted			DT Predicted	
	O	C		O	C
O	91	1		90	2
C	0	184		3	181

Table 4: Classification results according to the MLP and DT classifiers for the central versus peripheral nerve experiment.

	MLP	DT
Classification accuracy (%)	99.6%	98.2%
Sensitivity (%)	98.9%	97.8%
Specificity (%)	100%	98.4%
Positive rate (%)	100%	96.8%
Negative rate (%)	99.4%	98.9%

12
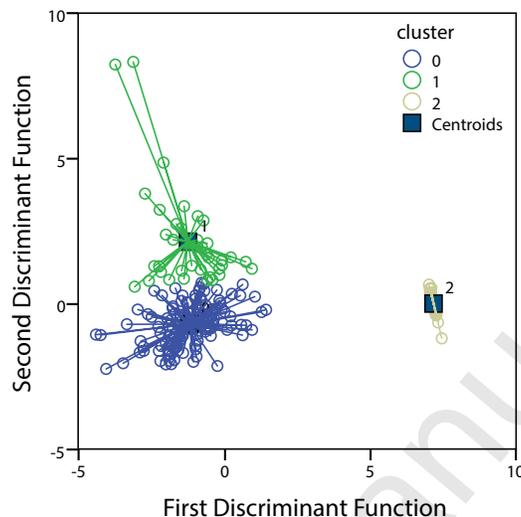
Figure 8: Representation of the three optic nerves clusters.

3.3. Intrafibre differences: different types of fibre within the optic and cochlear nerves

In the first phase of experimentation, we obtained five clusters of nerve fibres, for both the optic and cochlear nerves, using the k-means unsupervised algorithm. However, two of these classes had very few instances and whereby unbalanced classes would be created. Previous studies [20] have shown that three groups were required for a optimal solution for this classification. Therefore, in our experiments we "forced" the algorithm to produce an output with only three clusters and we observed that this change produced better results.

This process of analysis known as k-means allowed us to identify different groups of fibres in each type of nerve by creating these guided groups.

For each type of nerve, the centroids were identified with the main features of representative fibres in each group. In Tables 5 and 6 the values of these centroids are shown. By plotting the fibres forming each of these groups, it was revealed that they were sufficiently separated for the differences in their characteristics to become apparent. Figure 8 shows the distribution of fibres of the optic nerve using a discriminant analysis whereas Figure 9 is its equivalent to the cochlear nerve.

To assess that the cluster created were appropriated, we carried out several additional experiments. We again used the supervised MLP and DT algorithms. The results showed that the cluster chosen were correct since high accuracy was obtained for both the optic and cochlear nerves. In Table 7 we can see the four confusion matrices. It is shown that only a few of the fibres were incorrectly classified outside the diagonal in the matrix. Moreover, Table 8 presents the

13

Table 5: Distribution of the optic clusters and their centroids.

Cluster centroids (optic)				
		Cluster		
Attribute	Full Data	0	1	2
Number of cases	184	119	38	27
FIBRE DIAMETER	0.68	0.54	15.43	0.08
G-RATIO	0.54	0.45	0.48	1
R-PROPORTION	0.58	0.57	0.65	0.54
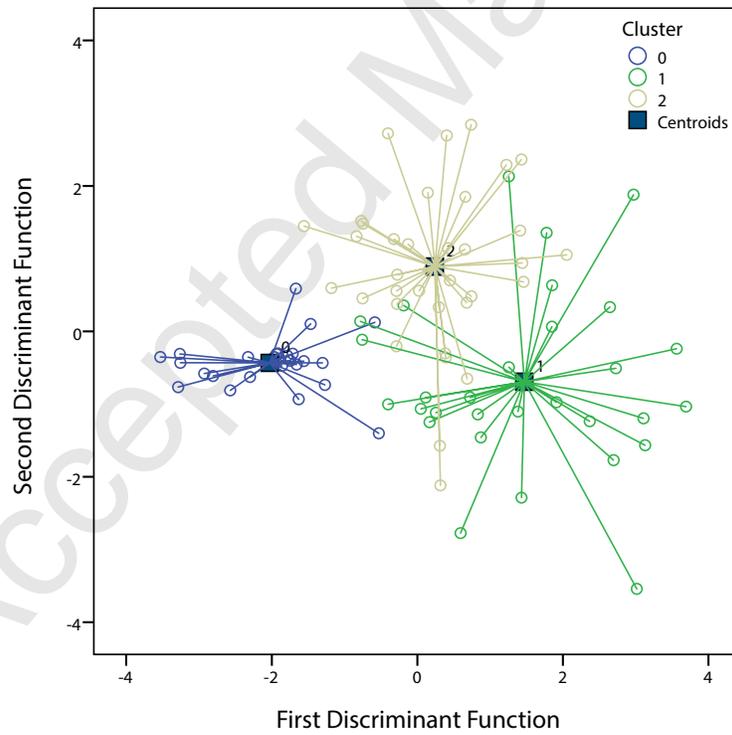
Figure 9: Representation of the three cochlear nerves clusters.

14

Table 6: Distribution of the cochlear clusters and their centroids.

Cluster centroids (cochlear)				
		Cluster		
Attribute	Full Data	0	1	2
Number of cases	92	26	30	36
AXON DIAMETER	1.57	1.75	1.81	1.24
MT NUMBER	52.43	30.92	70.76	52.69
NF DENSITY	112.02	45.92	123.81	149.95

Table 7: Definition of the confusion matrix for the clusters of the optic and cochlear nerves fibre. This table indicates the values for every measure of the MLP and DT classifiers. C1, C2, and C3 refer to the clusters obtained with the three type of nerve fibres.

	Optic							Cochlear					
	MLP				DT			MLP				DT	
Actual	Predicted				Predicted			Predicted				Predicted	
	C1	C2	C3		C1	C2	C3		C1	C2	C3	C1	C2	C3
C1	117	2	0		116	2	1		23	1	2	21	2	3
C2	0	38	0		4	34	0		0	29	1	2	28	0
C3	0	0	27		0	0	27		1	1	34	2	2	32

parameters that confirm the high accuracy obtained for the cluster classification.

Table 8: Equations according to the MLP and DT classifiers.

	Optic			Cochlear	
	MLP	DT		MLP	DT
Classification accuracy (%)	98.9%	96.2%		93.5%	88%
TP Rate (%)					
Cluster 0	98.3%	97.5%		88.5%	80.8%
Cluster 1	100%	89.5%		96.7%	93.3%
Cluster 2	100%	100%		94.4%	88.9%
TP Rate Precision (%)					
Cluster 0	100%	96.7%		95.8%	84%
Cluster 1	95%	94.4%		93.5%	87.5%
Cluster 2	100%	96.4%		91.9%	91.4%

Finally, Figures 10 and 11 show the accuracy of the decision trees obtained with the multi-level approach, providing a clear and comprehensive representation of how nerve fibres can be classified in groups once the first level has been established, CNS (optic) or PNS (cochlear).

4. Discussion

In this study, we adopted a bio-inspired multi-level classifier architecture of nerve fibres as a novel architecture approach for the automation of image anal-

15
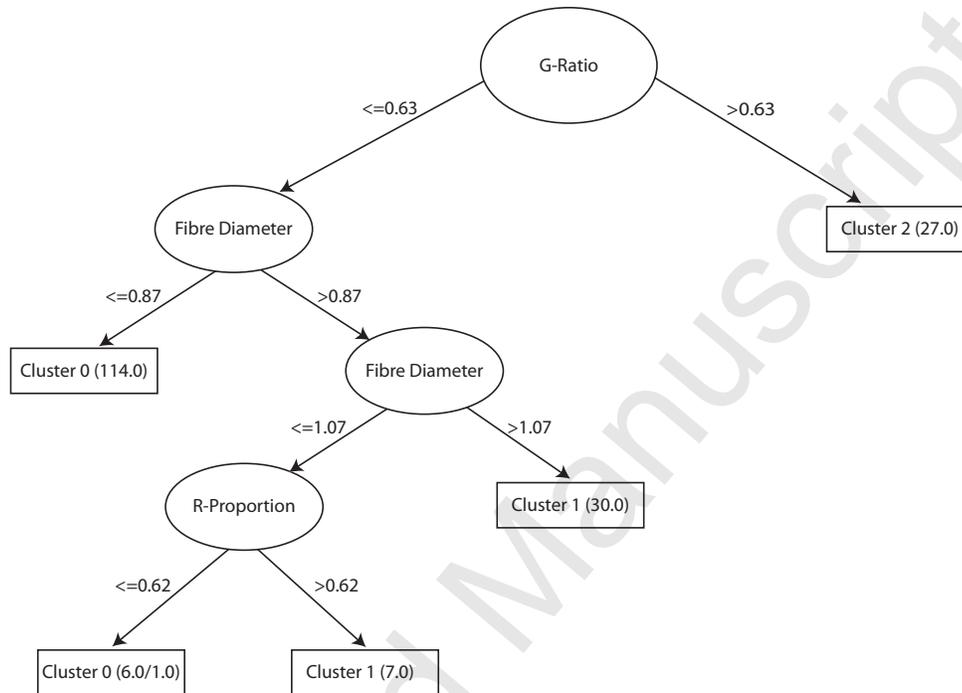
Figure 10: Decision tree representing the three optic-nerve clusters.
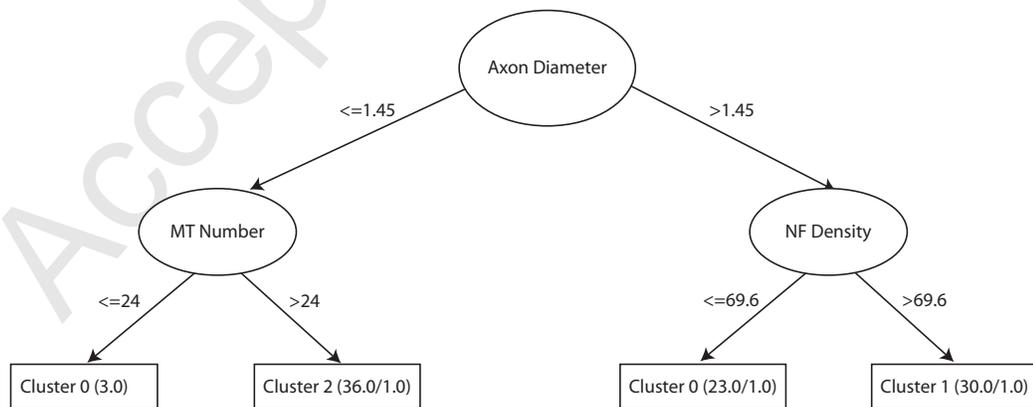
Figure 11: Decision tree representing the thee cochlear-nerve clusters.

16

ysis in clinical diagnosis. As a first step, we compared the accuracy of several artificial intelligence methods. Due to the complexity of biological systems, and particularly of the nervous system, it was not been possible to accomplish this task directly. The biological system of nerve fibres makes it necessary to develop a multi-level architecture because the classification task becomes complicated when we need to identify the location at the nerve fibre level (level 2), and we are not only concerned with whether the fibre belongs to the CNS or the PNS (level 1). Distinguishing between a central or a peripheral nerve fibre is a simple task for a trained pathologist who may be able to interpret the surrounding elements. However, for an automated system, the task becomes complicated due to the similar morphological features obtained from the morphometric analysis of the nerve fibres. In this study, we also identified the main morphometric parameters that define the type of fibre observed. Moreover, we demonstrated that the classification task only requires a small number of features, rendering it simpler than expected. This approach may lead to new studies based on different aspects of nerve-fibre development or the comparison of normal and pathological nerve fibre samples. In order to deal with this problem, we decided to implement a multi-level architecture. For the first level, we evaluated supervised methods such as DT and MLP, whereas for the second level we used unsupervised clustering techniques.

Artificial Intelligence methods have been used to improve a complex classification to distinguish between nerve fibres derived from central and peripheral nerves. In particular, we used two supervised techniques, MLP and DT, and an unsupervised one, K-Means clustering. The supervised methods classify the type of nerve fibre whereas the unsupervised one divides different types of fibres within the optic and cochlear nerves into clusters. Furthermore, to test the clusters created, we carried out several additional experiments with the MLP and DT algorithms. The AI methods achieved high accuracy, with MLP being more accurate (approximately 2% more, in general) than DT. However, this minor lower accuracy of DT is compensated by DT being more graphical and visual, which makes it easier to understand and interpret. K-Means clustering was also tested by testing the accuracy of the classification and prediction of these groups. Table 7 and 8 corroborate this unsupervised method with excellent results, in many cases with accuracy very close to 100%, which validates our proposed clustering.

Some AI methods have been effectively used in the field of the biological nervous systems in recent years, producing good results as well as reasonable expectations of ongoing improvements and evolution. Some of these methods have been presented by [76] and [77]. To the best of our knowledge, most of these studies used supervised methods to classify the different types of nerves and especially ANN. In our case, we contribute with this unsupervised method to create nerve-fibre clustering, as well as with the DT to render the results more visible and easier to interpret. The generalizable multi-level approach proposed in this study could improve the accuracy in comparison with our first approach.

One of the main objectives was to facilitate the routine tasks by automatization as well as to reduce costs in design and time. In this regard, a new

17

nerve fibre could be correctly classified between the optic and cochlear nerves. Then, it could be identified in the most suitable group, either in the optic or the cochlear nerve. The authors have experience in the medical field by applying several AI techniques in classification and prediction tasks with very good results [50] [51] [48].

Additionally, our architecture, characterized by complexity, generalization, and flexibility, can be extended to other biological control systems. To the best of our knowledge, this is the first time that a multilayer approach with AI methods (MLP, DT, and K-means) has been employed for the classification of nerve fibres.

In conclusion, the architecture developed in the present study allows for the correct classification of different types of nerve fibres. A multi-level structure is needed, in which supervised and unsupervised methods are used, in this order at different levels. This scheme improves classification accuracy and opens the possibility of its use in automated tasks. We demonstrated that the identification and classification of different types of nerve fibres can be carried out with a reduced number of characteristics.

In future research, one of the main objectives is to further the study of the nervous system, including other AI techniques and data mining, especially the mixed supervised-unsupervised techniques. This protocol, together with the incorporation of 3D imaging techniques, could improve accuracy and could facilitate the acquisition of more knowledge and experience in this domain. In addition, it should contribute to expanding the number of data repositories to improve storage, allowing the connection to data warehousing and big data, providing meaningful indicators and dashboards.

5. Acknowledgment

[1] H. F. Reinhardt, L. C. Henning, H. P. Rohr, Morphometrisch-ultrastrukturelle Untersuchungen am Hypophysenhinterlappen der Ratte nach Dehydratation, Zeitschrift für Zellforschung und Mikroskopische Anatomie 102 (2) (1969) 182–192. doi:10.1007/BF00335499.

18

[2] N. Cuenca, E. Fernandez, J. De Juan, J. Carreres, C. Iniguez, Postnatal development of microtubules and neurofilaments in the rat optic nerve: a quantitative study, Journal of Comparative Neurology 263 (4) (1987) 613–617.

[3] E. Fernández, N. Cuenca, J. R. Cerezo, J. De Juan, Visual experience during postnatal development determines the size of optic nerve axons., Neuroreport 5 (3) (1993) 365–7.

[4] N. Soltanpour, Y. Asghari Vostacolaee, M. Pourghasem, Comparison of Morphometric Aspects of Light and Electron Microscopy of the Hypoglossal Nerve between Young and Aged Male Wistar Rats., Cell journal 13 (4) (2012) 229–36.

[5] S. Sharma, B. Ray, D. Bhardwaj, A. K. Dwivedi, T. S. Roy, Age changes in the human oculomotor nerve A stereological study, Annals of Anatomy - Anatomischer Anzeiger 191 (3) (2009) 260–266. doi:10.1016/j.aanat.2009.02.008.

[6] A. Jeronimo, C. A. D. Jeronimo, O. A. R. Filho, L. S. Sanada, V. P. S. Fazan, A morphometric study on the longitudinal and lateral symmetry of the sural nerve in mature and aging female rats, Brain Research 1222 (2008) 51–60. doi:10.1016/j.brainres.2008.05.055.

[7] N. Nonaka, N. Goto, J. Goto, M. Shibata, M. Nakamura, Morphometric evaluation of the aging process in various human nerve fibers, Okajimas Folia Anatomica Japonica 85 (3) (2008) 103–106. doi:10.2535/ofaj.85.103.

[8] W. O. Cepurna, R. J. Kayton, E. C. Johnson, J. C. Morrison, Age related optic nerve axonal loss in adult Brown Norway rats, Experimental Eye Research 80 (6) (2005) 877–884. doi:10.1016/j.exer.2004.12.021.

[9] K. Sato, L. Sanada, R. da Ferreira, M. C. de Marco, J. Castania, H. Salgado, R. Nessler, V. P. Fazan, Renal nerve ultrastructural alterations in short term and long term experimental diabetes, BMC Neuroscience 15 (1) (2014) 5. doi:10.1186/1471-2202-15-5.

[10] H. Bagriyanik, N. Ersoy, C. Cetinkaya, E. Ikizoglu, D. Kutri, T. Ozcana, L. Kamanga, M. Kiray, The effects of resveratrol on chronic constriction injury of sciatic nerve in rats, Neuroscience Letters 561 (2014) 123–127. doi:10.1016/j.neulet.2013.12.056.

[11] Y. Kondo, H. Moriyama, S. Hirai, N. Qu, M. Itoh, The relationship between Bell's palsy and morphometric aspects of the facial nerve, European Archives of Oto-Rhino-Laryngology 269 (6) (2012) 1691–1695. doi:10.1007/s00405-011-1835-0.

[12] A. Hoke, M. Ray, Rodent Models of Chemotherapy-Induced Peripheral Neuropathy, ILAR Journal 54 (3) (2014) 273–281. doi:10.1093/ilar/ilt053.

19

[13] J. Reynaud, G. Cull, L. Wang, B. Fortune, S. Gardiner, C. F. Burgoyne, G. A. Cioffi, Automated Quantification of Optic Nerve Axons in Primate Glaucomatous and Normal EyesMethod and Comparison to Semi-Automated Manual Quantification, Investigative Opthalmology & Visual Science 53 (6) (2012) 2951. doi:10.1167/iovs.11-9274.

[14] H. S. Gasser, H. Grundfest, Axon diameters in relation to the spike dimensions and the conduction velocity in mammalian A fibers, Am. J. Physiol 127 (39) (1939) 414.

[15] J. B. Hursh, Conduction velocity and diameter of nerve fibers, Am. J. Physiol 127 (9) (1939) 131–139.

[16] M. V. Edds, Hypertrophy of nerve fibers to functionally overloaded muscles, The Journal of Comparative Neurology 93 (2) (1950) 259–275. doi:10.1002/cne.900930207.

[17] J. De Juan, C. Iniguez, J. Carreres, Number, diameter and distribution of the rat optic nerve fibers, Cells Tissues Organs 102 (3) (1978) 294–299.

[18] K. Fried, C. Hildebrand, Axon number and size distribution in the developing feline inferior alveolar nerve, Journal of the neurological sciences 53 (2) (1982) 169–180.

[19] C. A. Knox, E. Kokmen, P. J. Dyck, Morphometric alteration of rat myelinated fibers with aging, Journal of Neuropathology & Experimental Neurology 48 (2) (1989) 119–139.

[20] J. De Juan, N. Cuenca, C. Iñiguez, E. Fernández, Axon types classified by morphometric and multivariate analysis in the rat optic nerve, Brain research 585 (1) (1992) 431–434.

[21] B. Wattig, G. Schalow, M. Madauss, F. Heydenreich, R. Warzok, J. Cervós-Navarro, Acceleration of nerve and muscle regeneration by administration of nucleotides–electroneurophysiological and morphometrical investigations., Acta histochemica. Supplementband 42 (1991) 333–339.

[22] K. A. Sullivan, M. S. Brown, L. Harmon, D. A. Greene, Digital electron microscopic examination of human sural nerve biopsies, Journal of the Peripheral Nervous System 8 (4) (2003) 260–270. doi:10.1111/j.1085-9489.2003.03030.x.

[23] S. D. Demirer, I. Kepenekci, O. Evirgen, O. Birsen, A. Tuzuner, S. Karahuseyinoglu, M. Ozban, E. Kuterdem, The Effect of Polypropylene Mesh on the Ilioinguinal Nerve in Open Mesh Repair of Groin Hernia, Hernia Repair Sequelae 131 (2) (2010) 265–273. doi:10.1007/978-3-642-11541-7.

20

[24] W. A. H. Rushton, A theory of the effects of fibre size in medullated nerve, The Journal of Physiology 115 (1) (1951) 101–122. doi:10.1113/jphysiol.1951.sp004655.

[25] E. R. Arbuthnott, I. A. Boyd, K. U. Kalu, Ultrastructural dimensions of myelinated peripheral nerve fibres in the cat and their relation to conduction velocity, The Journal of Physiology 308 (1) (1980) 125–157. doi:10.1113/jphysiol.1980.sp013465.

[26] H. F. Webster, Myelinogenesis. Structural aspects., Neurosciences Research Program bulletin 9 (4) (1971) 470–477.

[27] E. R. Arbuthnott, K. J. Ballard, I. A. Boyd, K. U. Kalu, Quantitative study of the non-circularity of myelinated peripheral nerve fibres in the cat, The Journal of Physiology 308 (1) (1980) 99–123. doi:10.1113/jphysiol.1980.sp013464.

[28] K. Fried, C. Hildebrand, G. Erdélyi, Myelin sheath thickness and internodal length of nerve fibres in the developing feline inferior alveolar nerve, Journal of the Neurological Sciences 54 (1) (1982) 47–57. doi:10.1016/0022-510X(82)90217-9.

[29] K. Smith, W. Blakemore, J. Murray, R. Patterson, Internodal myelin volume and axon surface area, Journal of the Neurological Sciences 55 (2) (1982) 231–246. doi:10.1016/0022-510X(82)90103-4.

[30] R. L. Friede, W. Beuche, Combined scatter diagrams of sheath thickness and fibre calibre in human sural nerves: changes with age and neuropathy., Journal of Neurology, Neurosurgery & Psychiatry 48 (8) (1985) 749–756. doi:10.1136/jnnp.48.8.749.

[31] Z. Sahenk, S. T. Brady, Axonal tubulin and microtubules: Morphologic evidence for stable regions on axonal microtubules, Cell Motility and the Cytoskeleton 8 (2) (1987) 155–164. doi:10.1002/cm.970080207.

[32] E. Fernandez, N. Cuenca, J. De Juan, A useful programme in BASIC for axonal morphometry with introduction of new cytoskeletal parameters, Journal of neuroscience methods 39 (3) (1991) 271–289.

[33] W. Maxwell, D. Graham, Loss of Axonal Microtubules and Neurofilaments after Stretch-Injury to Guinea Pig Optic Nerve Fibers, Journal of Neurotrauma 14 (9) (1997) 603–614. doi:10.1089/neu.1997.14.603.

[34] D. R. Campion, R. L. Richardson, R. R. Kraeling, J. O. Reagan, Regulation of skeletal muscle development by the central nervous system in the fetal pig., Growth 42 (2) (1978) 189–204.

21

[35] K. Wakakuwa, M. Watanabe, T. Sugimoto, A. Washida, Y. Fukuda, An electron microscopic analysis of the optic nerve of the eastern chipmunk (Tamias sibiricus asiaticus): Total fiber count and retinotopic organisation, Vision Research 27 (11) (1987) 1891–1901. doi:10.1016/0042-6989(87)90055-1.

[36] G. Cull, G. A. Cioffi, J. Dong, L. Homer, L. Wang, Estimating normal optic nerve axon numbers in non-human primate eyes, Journal of glaucoma 12 (4) (2003) 301–306.

[37] X. Zhao, Z. Pan, J. Wu, G. Zhou, Y. Zeng, Automatic identification and morphometry of optic nerve fibers in electron microscopy images, Computerized Medical Imaging and Graphics 34 (3) (2010) 179–184.

[38] R. W. Williams, L. M. Chalupa, An analysis of axon caliber within the optic nerve of the cat: evidence of size groupings and regional organization, The journal of Neuroscience 3 (8) (1983) 1554–1564.

[39] D. E. Brooks, D. T. Strubbe, P. S. Kubilis, E. O. MacKay, D. A. Samuelson, K. N. Gelatt, Histomorphometry of the optic nerves of normal dogs and dogs with hereditary glaucoma, Experimental eye research 60 (1) (1995) 71–89.

[40] G. Vita, M. Santoro, G. Trombetta, L. Leonardi, C. Messina, A computer-assisted automatic method for myelinated nerve fiber morphometry, Acta neurologica scandinavica 85 (1) (1992) 18–22.

[41] Ying-Lun Fok, J. Chan, R. Chin, Automated analysis of nerve-cell images using active contour models, IEEE Transactions on Medical Imaging 15 (3) (1996) 353–368. doi:10.1109/42.500144.

[42] P. Campadelli, C. Gangai, F. Pasquale, Automated morphometric analysis in peripheral neuropathies, Computers in Biology and Medicine 29 (2) (1999) 147–156. doi:10.1016/S0010-4825(98)00051-1.

[43] A. P. D. da Silva, C. E. R. Jordão, V. P. S. Fazan, Peripheral nerve morphometry: Comparison between manual and semi-automated methods in the analysis of a small nerve, Journal of Neuroscience Methods 159 (1) (2007) 153–157. doi:10.1016/j.jneumeth.2006.06.012.

[44] I. Kononenko, Machine learning for medical diagnosis: history, state of the art and perspective, Artificial Intelligence in Medicine 23 (1) (2001) 89–109.

[45] E. Hadavandi, H. Shavandi, A. Ghanbari, S. Abbasian-Naghneh, Developing a hybrid artificial intelligence model for outpatient visits forecasting in hospitals, Applied Soft Computing 12 (2) (2012) 700–711. doi:10.1016/j.asoc.2011.09.018.

22

[46] Y. Wang, J. Li, J. Gu, Z. Zhou, Z. Wang, Artificial neural networks for infectious diarrhea prediction using meteorological factors in Shanghai (China), Applied Soft Computing 35 (2015) 280–290. doi:10.1016/j.asoc.2015.05.047.

[47] D. S. Kumar, G. Sathyadevi, S. Sivanesh, Decision Support System for Medical Diagnosis Using Data Mining, International Journal of Computer Science Issues 8 (3) (2011) 814–1694.

[48] D. Gil, J. L. Girela, J. De Juan, M. J. Gomez-Torres, M. Johnsson, Predicting seminal quality with artificial intelligence methods, Expert Systems with Applications 39 (16) (2012) 12564–12573. doi:10.1016/j.eswa.2012.05.028.

[49] J. L. Girela, D. Gil, M. Johnsson, M. J. Gomez-Torres, J. De Juan, Semen parameters can be predicted from environmental factors and lifestyle using artificial intelligence methods., Biology of reproduction 88 (4) (2013) 99. doi:10.1095/biolreprod.112.104653.

[50] D. Gil, M. Johnsson, J. M. Garcia Chamizo, A. S. Paya, D. R. Fernandez, Application of artificial neural networks in the diagnosis of urological dysfunctions, Expert Systems with Applications 36 (3) (2009) 5754–5760. doi:10.1016/j.eswa.2008.06.065.

[51] D. Gil, M. Johnsson, Using support vector machines in diagnoses of urological dysfunctions, Expert Systems with Applications 37 (6) (2010) 4713–4718. doi:10.1016/j.eswa.2009.12.055.

[52] A. Angelopoulou, A. Psarrou, J. Garcia-Rodriguez, S. Orts-Escolano, J. Azorin-Lopez, K. Revett, 3D reconstruction of medical images from slices automatically landmarked with growing neural models, Neurocomputing 150 (2015) 16–25. doi:10.1016/j.neucom.2014.03.078.

[53] D. Gil, M. Johnsson, J. M. García Chamizo, A. S. Paya, D. R. Fernández, Modelling of urological dysfunctions with neurological etiology by means of their centres involved, Applied Soft Computing 11 (8) (2011) 4448–4457. doi:10.1016/j.asoc.2011.05.029.

[54] K. Krishnan, Data Warehousing in the Age of Big Data, Morgan Kaufmann Publishers, 2013.

[55] J. J. Berman, Simple but Powerful Big Data Techniques, Elsevier, 2013. doi:10.1016/B978-0-12-404576-7.00008-3.

[56] J. Quinlan, Induction of Decision Trees, Machine Learning 1 (1) (1986) 81–106. doi:10.1023/A:1022643204877.

[57] J. R. Quinlan, C4. 5: programs for machine learning, Morgan Kaufmann, 1993.

23

[58] R. A. Breiman, L., Friedman, J., Stone, C. J., & Olshen, Classification and regression trees, Wadsworth International Group, 1984.

[59] M. Ture, F. Tokatli, I. Kurt, Using KaplanMeier analysis together with decision tree methods (C&RT, CHAID, QUEST, C4.5 and ID3) in determining recurrence-free survival of breast cancer patients, Expert Systems with Applications 36 (2) (2009) 2017–2026. doi:10.1016/j.eswa.2007.12.002.

[60] C.-C. Yang, S. O. Prasher, P. Enright, C. Madramootoo, M. Burgess, P. K. Goel, I. Callum, Application of decision tree technology for image classification using remote sensing data, Agricultural Systems 76 (3) (2003) 1101–1117. doi:10.1016/S0308-521X(02)00051-3.

[61] B. D. Ripley, Pattern recognition and neural networks, Cambridge university press, 1996.

[62] S. Haykin, Neural Networks: A Comprehensive Foundation, Prentice Hall PTR, 1998.

[63] C. M. Bishop, Neural Networks for Pattern Recognition., Vol. 92, Oxford Univ Pr, 1997. doi:10.2307/2965437.

[64] D. E. Rumelhart, G. E. Hinton, R. J. Williams, Learning representations by back-propagating errors, Nature 323 (6088) (1986) 533–536. doi:10.1038/323533a0.

[65] David J. C. MacKay, Information theory, inference and learning algorithms, Vol. 22, Cambridge university press, 2004. doi:10.1017/S026357470426043X.

[66] F. Aurenhammer, Voronoi diagrams—a survey of a fundamental geometric data structure, ACM Computing Surveys 23 (3) (1991) 345–405. doi:10.1145/116873.116880.

[67] R. O. Duda, P. E. Hart, D. G. Stork, Pattern classification, New York: John Wiley, 2001.

[68] L. Kaufman, P. J. Rousseeuw, Finding Groups in Data: : An Introduction to Cluster Analysis, Vol. 344 of Wiley Series in Probability and Statistics, John Wiley & Sons, Inc., Hoboken, NJ, USA, 1990. doi:10.1002/9780470316801.

[69] R. Xu, D. WunschII, Survey of Clustering Algorithms, IEEE Transactions on Neural Networks 16 (3) (2005) 645–678. doi:10.1109/TNN.2005.845141.

[70] A. K. Jain, Data clustering: 50 years beyond K-means, Pattern Recognition Letters 31 (8) (2010) 651–666. doi:10.1016/j.patrec.2009.09.011.

[71] S. K. Gupta, K. S. Rao, V. Bhatnagar, K-means Clustering Algorithm for Categorical Attributes, in: DataWarehousing and Knowledge Discovery, Springer, 1999, pp. 203–208. doi:10.1007/3-540-48298-9_22.

24

[72] E.-C. Chang, S.-C. Huang, H.-H. Wu, Using K-means method and spectral clustering technique in an outfitter's value analysis, Quality & Quantity 44 (4) (2010) 807–815. doi:10.1007/s11135-009-9240-0.

[73] R. Kohavi, F. Provost, Glossary of Terms, Machine Learning 30 (2/3) (1998) 271–274. doi:10.1023/A:1017181826899.

[74] I. H. Witten, E. Frank, M. A. Hall, C. J. Pal, Data Mining: Practical machine learning tools and techniques, Morgan Kaufmann, 2016.

[75] M. Pal, Factors Influencing the Accuracy of Remote Sensing Classification: A Comparative Study., University of Nottingham, 2002.

[76] E. Dudek-Dyduch, R. Tadeusiewicz, A. Horzyk, Neural network adaptation process effectiveness dependent of constant training data availability, Neurocomputing 72 (13-15) (2009) 3138–3149. doi:10.1016/j.neucom.2009.03.017.

[77] K. Polat, S. Kara, A. Güven, S. Güne?, Utilization of Discretization method on the diagnosis of optic nerve disease, Computer Methods and Programs in Biomedicine 91 (3) (2008) 255–264. doi:10.1016/j.cmpb.2008.04.009.

25

- Difficulties to distinguish between nerve fibers from central or peripheral Nervous System.

- The main aim is to distinguish nerve fibers based on their morphological characteristics.

- Our approach consists of a multilevel hierarchical classifier.

- This multilevel architecture comprises supervised and unsupervised methods.

- Our approach is characterized by complexity, generalization, and flexibility.

Digital Image Analysis

Level 0:
Supervised Methods

Level 1:
Unsupervised Methods

Multilevel Architecture